Solar Physics
DOI: 10.1007/•••••-•••-•••-••••-•

Solar Magneto-seismology with Magneto-acoustic Surface Waves in Asymmetric Magnetic Slabs Waveguides

Matthew Allcock[1] · **Robert Erdélyi**[1]

Abstract Solar magneto-seismology is a method used to approximate plasma parameters that are traditionally difficult to measure using observations of magneto-hydrodynamic waves. A magnetic slab can act as waveguide for magneto-acoustic waves that approximates magnetic structures in the Solar atmosphere. Asymmetry of the slab caused by different plasma parameters in each external region distorts both the eigenfrequencies and eigenfunctions of the system, that is both the temporal and spatial profiles of the waves that propagate along the slab. We present two novel diagnostic tools for solar magneto-seismology that use this distortion to estimate the slab magnetic field strength using the spatial distribution of magneto-acoustic surface waves: the *amplitude ratio* and the *minimum perturbation shift* methods. These methods can be used to approximate background parameters that are traditionally difficult to measure in inhomogeneous structures such as elongated magnetic bright points, prominences, and the locally slab-like magnetic structures above sunspot light bridges known as light walls, that may be locally approximated as slabs.

Keywords: Coronal Seismology; Magnetic fields, Photosphere; Waves, Magnetohydrodynamic; Waves, Modes.

1. Introduction

The emerging field of solar magneto-seismology (SMS) has become a crucial tool in developing our understanding of solar structures. By comparing observational measurements of magneto-hydrodynamic (MHD) waves to the wave solutions in inhomogeneous plasma models, we can make approximations of traditionally difficult-to-measure parameters such as the magnetic field strength and heat transport coefficient (Nakariakov and Verwichte, 2005; Arregui, 2012; De Moortel and Nakariakov, 2012). This in turn equips us with more realistic parameters for numerical simulations and give us a better understanding of conditions that lead to, for example instability, magnetic reconnection, and heating.

SMS techniques can be categorised as either temporal or spatial seismology. By temporal seismology we refer to methods that estimate a plasma parameter by using the observed frequency, or equivalently the period, of waves. By spatial seismology we refer to methods that estimate a

✉ R.Erdélyi
robertus@sheffield.ac.uk

[1] Solar Physics and Space Plasma Research Centre, School of Mathematics and Statistics, University of Sheffield, Hicks Building, Hounsfield Road, Sheffield, S3 7RH, UK.

plasma parameter by comparing the observed spatial and/or temporal wave power distribution with the eigenfunctions from a theoretical model.

Several temporal seisology methods have been employed successfully. Rosenberg (1970) first suggested that the frequency of oscillations, observed through the fluctuation of synchrotron radiation due to the presence of MHD waves, could be used to diagnose background parameters. Further theoretical development has led to more sophisticated temporal methods including local coronal magnetic field strength estimates using standing kink modes in coronal loops by Nakariakov and Ofman (2001), and using slow sausage and kink modes by Erdélyi and Taroyan (2008). The ratio of periods of the fundamental and the first harmonic standing kink mode and its dependence on density stratification has also been well studied (Banerjee *et al.*, 2007; Erdélyi, Hague, and Nelson, 2014).

Spatial seismology techniques have more recently started demonstrating their efficacy in estimating solar parameters. Uchida (1970) estimated the coronal magnetic structure by comparing Moreton wave observations with the theoretical influence that the coronal magnetic field has on the shape of the Moreton wavefront. More recent eigenfunction methods include utilising the anti-node shift of standing modes in a magnetic flux tube to diagnose its inhomogeneous density stratification (Verth *et al.*, 2007; Erdélyi, Hague, and Nelson, 2014).

In the present work, we derive two novel analytical tools for spatial seismology that use an asymmetric slab waveguide to approximate background parameters. This has applications to solar atmospheric structures that are locally slab-like which have been observed to guide MHD oscillations, such as elongated magnetic bright points, prominences, and the locally slab-like magnetic structures above sunspot light bridges known as light walls (Arregui, Oliver, and Ballester, 2012; Yang *et al.*, 2017; Zhang *et al.*, 2017).

This is an application of the linear wave analysis of asymmetric magnetic slabs completed by Allcock and Erdélyi (2017). A magnetic slab, with non-magnetic, but asymmetric density and temperatures outside the slab has eigenmodes which can be described as either quasi-sausage or quasi-kink. For quasi-sausage (quasi-kink) modes, the oscillations on each slab interface are in anti-phase (phase). They differ from traditional (symmetric) sausage and kink modes by the fact that they are asymmetric about the center of the slab due to the amplitude of oscillation on each interface being unequal. This results in quasi-kink modes not necessarily retaining their cross-sectional area and quasi-sausage modes not necessarily having reflection symmetric about the centre line of the slab. The spatial distribution of these waves across the slab, and therefore the extent to which they are modified from the traditional sausage and kink modes, is dependent on the background plasma parameters. Consequently, we can use the spatial distribution of these waves to diagnose certain background parameters. This is the focus of the present paper, to derive expressions for these quantities and discuss the application to SMS.

2. Amplitude ratio

The aim of this section is to derive an expression for the ratio of the oscillation on each interface of an asymmetric magnetic slab in terms of the wave and plasma parameters of the system.

Consider an inviscid, plasma structured by two parallel interfaces separating the plasma into three regions along the $\widehat{\boldsymbol{x}}$-direction. In each region the plasma is uniform and the central region, known as the slab, has a uniform magnetic field, $\boldsymbol{B} = B_0\widehat{\boldsymbol{z}}$. The plasma adjacent to the slab on each side is non-magnetic. The density, pressure, and sound speed within the slab are denoted by ρ_0, p_0, and c_0, respectively, and in the external plasma they are subscripted by 1 and 2, respectively. For more information about the equilibrium conditions, see Allcock and Erdélyi,

2017. In the aforementioned work, it was shown that trapped magneto-acoustic modes propagating along an asymmetric magnetic slab have velocity perturbation in the $\widehat{\boldsymbol{x}}$-direction given by $v_x(x,y,z,t) = \widehat{v}_x(x)e^{i(kz-\omega t)}$, where ω and k are the angular frequency and wavenumber, and

$$\widehat{v}_x(x) = \begin{cases} A(\cosh m_1 x + \sinh m_1 x) & \text{if } x < -x_0, \\ B\cosh m_0 x + C\sinh m_0 x & \text{if } |x| \le x_0, \\ D(\cosh m_2 x - \sinh m_2 x) & \text{if } x > x_0, \end{cases} \tag{2.1}$$

where

$$m_0^2 = \frac{(k^2 v_{\rm A}^2 - \omega^2)(k^2 c_0^2 - \omega^2)}{(c_0^2 + v_{\rm A}^2)(k^2 c_{\rm T}^2 - \omega^2)}, \qquad c_{\rm T}^2 = \frac{c_0^2 v_{\rm A}^2}{c_0^2 + v_{\rm A}^2}, \tag{2.2}$$

$$m_j^2 = k^2 - \frac{\omega^2}{c_j^2}, \quad \text{for } j = 1, 2, \tag{2.3}$$

and A, B, C, and D are arbitrary constants (with respect to x). These constants can be determined, to within one degree of freedom, using the boundary conditions of continuity in total (kinetic plus magnetic) pressure and transversal velocity component across the slab boundaries at $x = \pm x_0$. Applying these four boundary conditions retrieves four coupled linear homogeneous algebraic equations in the four unknowns:

$$\begin{pmatrix} c_1 - s_1 & -c_0 & s_0 & 0 \\ 0 & c_0 & s_0 & s_2 - c_2 \\ \Lambda_1(c_1 - s_1) & \Lambda_0 s_0 & -\Lambda_0 c_0 & 0 \\ 0 & \Lambda_0 s_0 & \Lambda_0 c_0 & -\Lambda_2(s_2 - c_2) \end{pmatrix} \begin{pmatrix} A \\ B \\ C \\ D \end{pmatrix} = \begin{pmatrix} 0 \\ 0 \\ 0 \\ 0 \end{pmatrix}, \tag{2.4}$$

where

$$\Lambda_0 = -\frac{i\rho_0(k^2 v_{\rm A}^2 - \omega^2)}{m_0 \omega}, \quad \Lambda_1 = \frac{i\rho_1 \omega}{m_1}, \quad \text{and} \quad \Lambda_2 = \frac{i\rho_2 \omega}{m_2}, \tag{2.5}$$

and $c_i = \cosh m_i x_0$ and $s_i = \sinh m_i x_i$ for $i = 0, 1, 2$. Ensuring that this matrix has a vanishing determinant gives us the dispersion relation:

$$(\Lambda_0 c_0 + \Lambda_2 s_0)(\Lambda_0 s_0 + \Lambda_1 c_0) + (\Lambda_0 c_0 + \Lambda_1 s_0)(\Lambda_0 s_0 + \Lambda_2 c_0) = 0. \tag{2.6}$$

By satisfying this relation, we gain one degree of freedom in the system of Equations (2.4) which allows one of the constants B or C to be arbitrary. This gives us two types of solution: quasi-sausage and quasi-kink modes.

Firstly, for quasi-sausage modes, by letting C be arbitrary the other constants A, B, and D can be determined as

$$A = \frac{1}{c_1 - s_1}(Bc_0 - Cs_0), \tag{2.7}$$

$$D = \frac{1}{c_2 - s_2}(Bc_0 + Cs_0), \tag{2.8}$$

$$\text{where} \quad B = \frac{\Lambda_0 c_0 + \Lambda_1 s_0}{\Lambda_0 s_0 + \Lambda_1 c_0} C = -\frac{\Lambda_0 c_0 + \Lambda_2 s_0}{\Lambda_0 s_0 + \Lambda_2 c_0} C. \tag{2.9}$$

The second formulation of B in equation (2.9) is found by utilising the dispersion relation. A substitution of these values, using the first form of B in Equation (2.9), into the velocity solution,

equation (2.1), evaluated at the slab boundaries, yields

$$\widehat{v}_x(x_0) = Bc_0 + Cs_0 = \frac{2\Lambda_1 + \Lambda_0\left(\tau_0 + \frac{1}{\tau_0}\right)}{\Lambda_0 + \Lambda_1\frac{1}{\tau_0}}Cc_0, \tag{2.10}$$

$$\widehat{v}_x(-x_0) = Bc_0 - Cs_0 = \frac{\Lambda_0}{\Lambda_0 + \Lambda_1\frac{1}{\tau_0}}C/s_0, \tag{2.11}$$

where $\tau_0 = \tanh m_0 x_0$. similarly, using the second form of B in Equation (2.9) yields

$$\widehat{v}_x(x_0) = \frac{-\Lambda_0}{\Lambda_0 + \Lambda_2\frac{1}{\tau_0}}C/s_0, \tag{2.12}$$

$$\widehat{v}_x(-x_0) = \frac{-2\Lambda_2 - \Lambda_0\left(\tau_0 + \frac{1}{\tau_0}\right)}{\Lambda_0 + \Lambda_2\frac{1}{\tau_0}}Cc_0. \tag{2.13}$$

These forms are equivalent. The horizontal velocity perturbation amplitude, $\widehat{v}_x$, is the *signed* amplitude, where a positive (negative) value indicates perturbation in the positive (negative) $\widehat{\boldsymbol{x}}$-direction.

Secondly, for quasi-kink modes, by letting B be arbitrary, the other constants A, C, and D can be determined in terms of B as

$$A = \frac{1}{c_1 - s_1}(Bc_0 - Cs_0), \tag{2.14}$$

$$D = \frac{1}{c_2 - s_2}(Bc_0 + Cs_0), \tag{2.15}$$

$$\text{where} \quad C = \frac{\Lambda_0 s_0 + \Lambda_1 c_0}{\Lambda_0 c_0 + \Lambda_1 s_0}B = -\frac{\Lambda_0 s_0 + \Lambda_2 c_0}{\Lambda_0 c_0 + \Lambda_2 s_0}B. \tag{2.16}$$

A substitution of these values, using the first form of C in Equation (2.16), into Equation (2.1), evaluated at the slab boundaries ($x = \pm x_0$), yields

$$\widehat{v}_x(x_0) = \frac{2\Lambda_1 + \Lambda_0\left(\tau_0 + \frac{1}{\tau_0}\right)}{\Lambda_0 + \Lambda_1\tau_0}Bs_0, \tag{2.17}$$

$$\widehat{v}_x(-x_0) = \frac{\Lambda_0}{\Lambda_0 + \Lambda_1\tau_0}B/c_0. \tag{2.18}$$

Using the second form of C in Equation (2.16) yields

$$\widehat{v}_x(x_0) = \frac{\Lambda_0}{\Lambda_0 + \Lambda_2\tau_0}B/c_0, \tag{2.19}$$

$$\widehat{v}_x(-x_0) = \frac{2\Lambda_2 + \Lambda_0\left(\tau_0 + \frac{1}{\tau_0}\right)}{\Lambda_0 + \Lambda_2\tau_0}Bs_0. \tag{2.20}$$

We now define the *amplitude ratio*, $R_\mathrm{A} := \widehat{\xi}_x(x_0)/\widehat{\xi}_x(-x_0)$, as the ratio of the amplitude of oscillation of the left interface ($x = x_0$) to that of the right interface ($x = -x_0$) (Figure 1). Given that $\widehat{\xi}_x(x) = i\widehat{v}_x(x)/\omega$, we also have $R_\mathrm{A} = \widehat{v}_x(x_0)/\widehat{v}_x(-x_0)$. Firstly, using equations (2.11) and

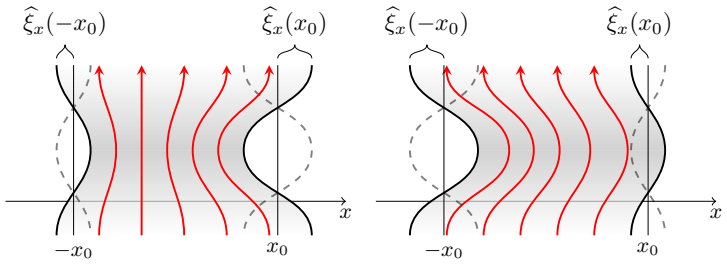

Figure 1. Illustration of the difference in amplitude of oscillation on each boundary of the slab for (a) quasi-sausage and (b) quasi-kink modes. The ratio of the amplitudes can be used as a diagnostic tool.

(2.12), the amplitude ratio for quasi-sausage modes is

$$\begin{aligned} R_A &= -\frac{\Lambda_0 + \Lambda_1 \frac{1}{\tau_0}}{\Lambda_0 + \Lambda_2 \frac{1}{\tau_0}} \\ &= -\frac{\rho_1 m_2}{\rho_2 m_1}\left[\frac{(k^2 v_{\rm A}^2 - \omega^2) m_1 \frac{\rho_0}{\rho_1} - \omega^2 m_0 \frac{1}{\tanh m_0 x_0}}{(k^2 v_{\rm A}^2 - \omega^2) m_2 \frac{\rho_0}{\rho_2} - \omega^2 m_0 \frac{1}{\tanh m_0 x_0}}\right]. \end{aligned} \tag{2.21}$$

Using equations (2.18) and (2.19), the corresponding expression for quasi-kink modes can be obtained, namely

$$\begin{aligned} R_{\rm A} &= \frac{\Lambda_0 + \Lambda_1 \tau_0}{\Lambda_0 + \Lambda_2 \tau_0} \\ &= \frac{\rho_1 m_2}{\rho_2 m_1}\left[\frac{(k^2 v_{\rm A}^2 - \omega^2) m_1 \frac{\rho_0}{\rho_1} - \omega^2 m_0 \tanh m_0 x_0}{(k^2 v_{\rm A}^2 - \omega^2) m_2 \frac{\rho_0}{\rho_2} - \omega^2 m_0 \tanh m_0 x_0}\right]. \end{aligned} \tag{2.22}$$

As expected, equations (2.21) and (2.22) reduce to $R_{\rm A} = -1$ and $R_{\rm A} = 1$ for sausage and kink modes, respectively, when the slab is symmetric.

The following subsections give the analytical solution for the Alfvén speed, $v_{\rm A}$, of equations (2.21) and (2.22) under the thin slab, wide slab, incompressible plasma, and low-beta approximations. To obtain an approximation for the Alfvén speed analytically, an approximation such as these must be applied. Note that we restrict the analysis to surface modes only, thereby omitting body modes, because the eigenfrequencies and eigenfunctions of body modes are not significantly effected by asymmetry in the external plasma (Allcock and Erdélyi, 2017).

2.1. Thin slab approximation

In the thin slab approximation, $kx_0 \ll 1$, it has been shown that $m_0 x_0 \ll 1$ for surface modes (Roberts, 1981b). Therefore, $\tanh m_0 x_0 \approx m_0 x_0$ and the amplitude ratio for a quasi-sausage surface mode in a thin slab reduces to

$$R_{\rm A} = -\frac{\rho_1 m_2}{\rho_2 m_1}\left[\frac{(k^2 v_{\rm A}^2 - \omega^2) m_1 x_0 \frac{\rho_0}{\rho_1} - \omega^2}{(k^2 v_{\rm A}^2 - \omega^2) m_2 x_0 \frac{\rho_0}{\rho_2} - \omega^2}\right], \tag{2.23}$$

which has analytical solutions

$$v_{\rm A}^2 = \frac{\omega^2}{k^2}\left[1 + \frac{1}{x_0}\left(\frac{R_{\rm A}\frac{\rho_2}{\rho_0 m_2} + \frac{\rho_1}{\rho_0 m_1}}{R_{\rm A}+1}\right)\right]. \tag{2.24}$$

The amplitude ratio for a thin slab quasi-kink surface mode reduces to

$$R_{\rm A} = \frac{\rho_1 m_2}{\rho_2 m_1}\left[\frac{(k^2 v_{\rm A}^2 - \omega^2)m_1\frac{\rho_0}{\rho_1} - \omega^2 m_0^2 x_0}{(k^2 v_{\rm A}^2 - \omega^2)m_2\frac{\rho_0}{\rho_2} - \omega^2 m_0^2 x_0}\right], \tag{2.25}$$

which has analytical solutions

$$v_{\rm A}^2 = \frac{\omega^2}{k^2}\left[\frac{c_0^2}{c_0^2 - \frac{\omega^2}{k^2}} + k^2 x_0\left(\frac{R_{\rm A}\frac{\rho_2}{\rho_0 m_2} - \frac{\rho_1}{\rho_0 m_1}}{R_{\rm A}-1}\right)\right]. \tag{2.26}$$

In a thin asymmetric slab, the fast quasi-kink surface mode degenerates due to a cut-off by the external sound speeds becoming distinct (Allcock and Erdélyi, 2017) and the slow quasi-kink surface mode has a phase speed that approaches zero in the thin slab limit. Therefore, to a good approximation, the phase speed is much less than the internal sound speed ($\omega/k \ll c_0$) therefore Solution (2.26) simplifies to

$$v_{\rm A}^2 = \frac{\omega^2}{k^2}\left[1 + k^2 x_0\left(\frac{R_{\rm A}\frac{\rho_2}{\rho_0 m_2} - \frac{\rho_1}{\rho_0 m_1}}{R_{\rm A}-1}\right)\right]. \tag{2.27}$$

2.2. Wide slab approximation

The wide slab approximation applies when the slab width is much larger than the wavelength, that is $kx_0 \gg 1$. To understand the properties of the eigenfunctions of the asymmetric slab system in the wide slab approximation, we must return to the dispersion relation, Equation (2.6). For surface modes in the slab, the wide slab approximation implies that $m_0 x_0 \gg 1$, therefore $\sinh m_0 x_0 \approx \cosh m_0 x_0 \approx 1$ (Roberts, 1981b). Under this approximation, the dispersion relation, Equation (2.6), becomes

$$(\Lambda_0 + \Lambda_1)(\Lambda_0 + \Lambda_2) = 0, \tag{2.28}$$

which gives us two families of solutions, one satisfying $\Lambda_0 + \Lambda_1 = 0$ and the other satisfying $\Lambda_0 + \Lambda_2 = 0$. These are equivalent to

$$(k^2 v_{\rm A}^2 - \omega^2)m_j\frac{\rho_0}{\rho_j} - \omega^2 m_0 = 0, \tag{2.29}$$

for $j = 1, 2$, respectively. This equation is the same as the dispersion relation governing surface waves along a single interface between a magnetised and a non-magnetised plasma (Roberts, 1981a). Hence, the surface mode solutions of a wide asymmetric slab are just the surface modes that propagate along each interface independently. This makes intuitive sense considering that as the slab is widened the interfaces will have diminishing influence on each other, until each interface oscillates independently with its own characteristic frequency.

This is analogous to the mechanical example introduced by Allcock and Erdélyi, 2017. Consider two masses connected by a spring, with spring constant k_0, and each mass is also connected to a fixed wall on each side by springs with spring constants k_1 and k_2, respectively (Figure 2). When the middle spring has spring constant $k_0 \neq 0$, there are two modes, an in-phase mode

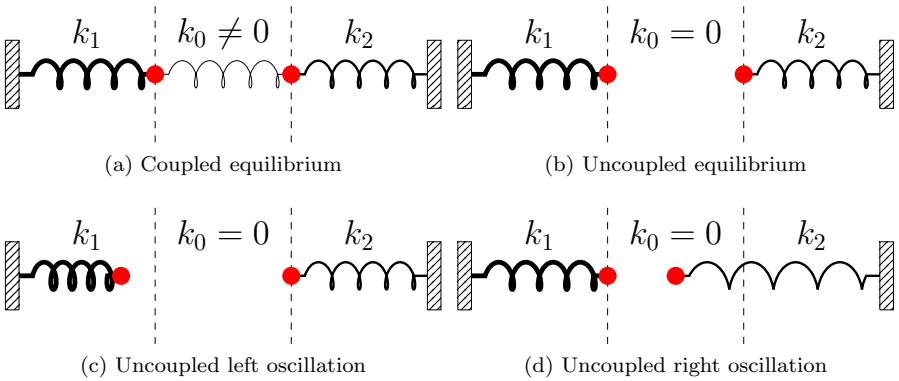

Figure 2. Mechanical example showing weak and zero coupling between the masses. This provides an analogy to the wide slab approximation of an asymmetric magnetic slab, in which case the interfaces on each side of the slab oscillate independently.

(analogous to kink modes in a slab) and an in-antiphase mode (analogous to sausage modes in a slab) (Allcock and Erdélyi, 2017). When the two masses are decoupled by removing the middle spring, equivalently setting $k_0 = 0$, each mass oscillates independently at the natural frequency of that side of the spring-mass system. This decoupling provides a good analogy to the wide slab limit for the magnetic slab. Each interface can oscillate at its own natural frequency, independent of the other interface. Given that we are considering magneto-acoustic waves, there are two restoring forces, the magnetic tension force and the pressure gradient force, which means that each independent interface has two natural frequencies (depending on the parameters of the system, there can be 0, 1, or 2 frequencies), corresponding to the fast and slow magneto-acoustic modes.

With this understanding of the modes in the wide slab limit, the amplitude ratio, $R_{\rm A}$, is either 0 or *undefined*, depending on which interface the wave is propagating and is therefore not useful for magneto-seismology.

2.3. Incompressible Approximation

If the plasma in each region is incompressible, the sound speeds become unbounded, so that $m_j \approx k$ for $j = 0, 1, 2$. Under this approximation, the amplitude ratio for quasi-sausage modes (top) and quasi-kink modes (bottom) reduces to

$$R_{\rm A} = \begin{pmatrix} - \\ + \end{pmatrix} \frac{\rho_1}{\rho_2} \left[\frac{(k^2 v_{\rm A}^2 - \omega^2) k \frac{\rho_0}{\rho_1} - \omega^2 k \begin{pmatrix} \coth \\ \tanh \end{pmatrix} (kx_0)}{(k^2 v_{\rm A}^2 - \omega^2) k \frac{\rho_0}{\rho_2} - \omega^2 k \begin{pmatrix} \coth \\ \tanh \end{pmatrix} (kx_0)} \right]. \tag{2.30}$$

These equations have solutions for $v_{\rm A}$ given by

$$v_{\rm A}^2 = \frac{\omega^2}{k^2} \left[1 + \left(\frac{R_{\rm A} \frac{\rho_2}{\rho_0} \begin{pmatrix} + \\ - \end{pmatrix} \frac{\rho_1}{\rho_0}}{R_{\rm A} \begin{pmatrix} + \\ - \end{pmatrix} 1} \right) \begin{pmatrix} \coth \\ \tanh \end{pmatrix} (kx_0) \right]. \tag{2.31}$$

2.4. Low-Beta Approximation

For a low-beta plasma ($\beta = 2\mu_0 p_0 / B_0^2 \ll 1$), where the magnetic pressure dominates the plasma pressure, the Alfvén speed, $v_{\rm A}$, dominates the internal sound speed, c_0, so that $m_0^2 \approx k^2 - \omega^2 / v_{\rm A}^2$.

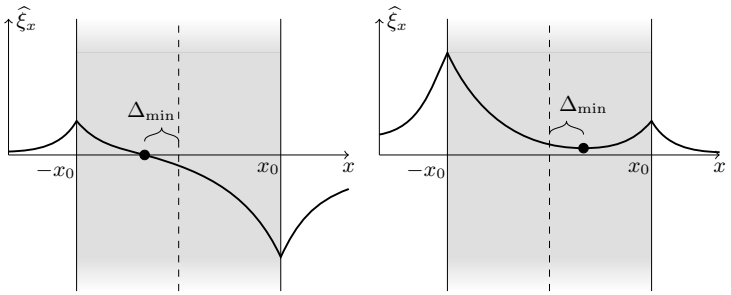

Figure 3. Illustration of the minimum perturbation shift within the slab for (a) quasi-sausage and (b) quasi-kink modes. The minimum perturbation shift can be used as a diagnostic tool.

For waves with phase speed much less than the Alfvén speed, a further approximation of $m_0^2 \approx k^2$ can be made, in which case the amplitude ratio for quasi-sausage modes (top) and quasi-kink modes (bottom) reduces to

$$R_{\rm A} = \begin{pmatrix} - \\ + \end{pmatrix} \frac{\rho_1 m_2}{\rho_2 m_1} \left[\frac{(k^2 v_{\rm A}^2 - \omega^2) m_1 \frac{\rho_0}{\rho_1} - \omega^2 k \begin{pmatrix} \coth \\ \tanh \end{pmatrix} (k x_0)}{(k^2 v_{\rm A}^2 - \omega^2) m_2 \frac{\rho_0}{\rho_2} - \omega^2 k \begin{pmatrix} \coth \\ \tanh \end{pmatrix} (k x_0)} \right]. \tag{2.32}$$

These equations can be solved for $v_{\rm A}$ to give

$$v_{\rm A}^2 = \frac{\omega^2}{k^2} \left[1 + k \left(\frac{\frac{\rho_1}{\rho_0 m_1} \begin{pmatrix} + \\ - \end{pmatrix} R_{\rm A} \frac{\rho_2}{\rho_0 m_2}}{1 \begin{pmatrix} + \\ - \end{pmatrix} R_{\rm A}} \right) \begin{pmatrix} \coth \\ \tanh \end{pmatrix} (k x_0) \right]. \tag{2.33}$$

We will return to a discussion of the inversion of the amplitude ratio in Section 4.

3. Shift of minimum perturbation

A second spatial seismology technique uses the shift in the position of minimum wave power from the centre of the slab due to the asymmetry in the external plasma regions as a diagnostic parameter for the slab Alfvén speed.

The position of minimum wave power for a symmetric sausage or kink mode is at the central line of the slab, at $x = 0$. We define $\Delta_{\min}$ to be the displacement (from the central line) of the position of minimum wave power inside an asymmetric magnetic slab (Figure 3). For quasi-sausage modes, $\Delta_{\min}$ is the solution to $\widehat{v}_x(x) = 0$ under the constraint $|x| < x_0$, and for quasi-kink modes, $\Delta_{\min}$ is the solution to $\mathrm{d}\widehat{v}_x(x)/\mathrm{d}x = 0$ under the same constraint $|x| < x_0$. The constraint restricts the solutions to being within the slab.

Firstly, for quasi-sausage modes, using the solution for the transversal velocity amplitude given by Equation (2.1) and the expressions for the variables within given by equation (2.9), the shift of minimum perturbation can be calculated as follows. The solution for the transversal velocity amplitude within the slab is

$$\widehat{v}_x(x) = B \cosh m_0 x + C \sinh m_0 x = 0, \tag{3.1}$$

where B is given by equation (2.9) and C is arbitrary. This equation is solved for x to give

$$x = \frac{1}{m_0} \tanh^{-1}\left(-\frac{B}{C}\right). \tag{3.2}$$

therefore the shift of minimum perturbation is

$$\Delta_{\min} = \frac{1}{m_0} \tanh^{-1}\left(-\frac{(k^2 {v_{\rm A}}^2 - \omega^2) m_1 \frac{\rho_0}{\rho_1} - \omega^2 m_0 \tanh m_0 x_0}{(k^2 {v_{\rm A}}^2 - \omega^2) m_1 \frac{\rho_0}{\rho_1} \tanh m_0 x_0 - \omega^2 m_0}\right). \tag{3.3}$$

Similarly, for quasi-kink modes, using Equations (2.1) and (2.16) we calculate the shift of minimum perturbation to be

$$\Delta_{\min} = \frac{1}{m_0} \coth^{-1}\left(-\frac{(k^2 {v_{\rm A}}^2 - \omega^2) m_1 \frac{\rho_0}{\rho_1} - \omega^2 m_0 \tanh m_0 x_0}{(k^2 {v_{\rm A}}^2 - \omega^2) m_1 \frac{\rho_0}{\rho_1} \tanh m_0 x_0 - \omega^2 m_0}\right). \tag{3.4}$$

It appears that expressions (3.3) and (3.4) for the minimum perturbation shifts depend on the parameters in the slab (subscript 0), the left external plasma (subscript 1), but not on the parameters of the right external plasma (subscript 2). However, the dependence on the right external plasma is implicit in the determination of the eigenfrequency ω when solving the dispersion relation.

The concept of minimum perturbation shift is exclusive to surface modes. The eigenfunctions of surface modes in a magnetic slab depend much more on the plasma parameters, such as the density, than body modes (Allcock and Erdélyi, 2017). This makes intuitive sense given that the energy in a surface mode is localised to the boundaries of the slab whereas the energy in a body mode is largely isolated within the slab. There is a quantifiable shift in the spatial nodes and anti-nodes in body mode perturbations within a slab due to changing external plasma parameters, however it is so small that is would not be an effective observational tool.

Akin to the amplitude ratio method for solar magneto-seismology prescribed in Section 2, we can solve equation (3.3) or (3.4) for the Alfvén speed, $v_{\rm A}$, to achieve an approximation for the magnetic field strength of inhomogeneous solar magnetic structures. This can be done either numerically, using an iterative root finding method, or analytically, under an appropriate approximation. In each of the following subsections, we make an inversion for the Alfvén speed, $v_{\rm A}$ under an approximation.

3.1. Thin slab approximation

As noted in Section 2.1, under the thin slab approximation, that is $kx_0 \ll 1$, we have $m_0 x_0 \ll 1$ for surface modes. By definition $|\Delta_{\min}| < x_0$, therefore $m_0 |\Delta_{\min}| \ll 1$, so that $\tanh m_0 \Delta_{\min} \approx m_0 \Delta_{\min}$. Firstly, for quasi-sausage modes, Equation (3.3) can be solved for $v_{\rm A}$ to give

$$v_{\rm A}^2 = \frac{\omega^2}{k^2}\left[\frac{\rho_1}{\rho_0 m_1}(x_0 + \Delta_{\min}) + \frac{1}{1 + (\omega/kc_0)^2} + k^2 x_0 \Delta_{\min}\right]. \tag{3.5}$$

For quasi-kink modes in a thin slab, Equation (3.4) can be solved for $v_{\rm A}$ to give

$$v_{\rm A}^2 = \frac{\omega^2}{k^2}\left[\frac{-b \pm \sqrt{b^2 - 4ac}}{2a}\right], \tag{3.6}$$

where

$$a = m_1 \frac{\rho_0}{\rho_1}(k^2 c_0^2 - \omega^2)(x_0 + \Delta_{\min}), \tag{3.7}$$

$$b = -m_1 \frac{\rho_0}{\rho_1}(2k^2 c_0^2 - \omega^2)(x_0 + \Delta_{\min}) - (k^2 c_0^2 - \omega^2), \tag{3.8}$$

$$c = c_0^2 m_1 \frac{\rho_0}{\rho_1}(x_0 + \Delta_{\min}) + c_0^2 + \omega^2 x_0 \Delta_{\min}. \tag{3.9}$$

3.2. Wide slab approximation

The concept of minimum perturbation shift is ill-defined under the wide slab approximation. In the wide slab approximation, each interface oscillates independently at its own eigenfrequency. Therefore the nomenclature of quasi-sausage and quasi-kink mode breaks down. In the wide slab limit, the eigenfunctions have no local minimum in the slab, instead the perturbations are evanescent away from the oscillating interface, therefore there is no local minimum of wave power within the slab.

3.3. Incompressible approximation

When the plasma is incompressible, the sound speeds are unbounded, so that $m_j = k$, for $j = 0, 1, 2$. The minimum perturbation shift for a quasi-sausage mode (top) and quasi-kink (bottom) in an incompressible slab is

$$\Delta_{\min} = \frac{1}{k} \begin{pmatrix} \tanh^{-1} \\ \coth^{-1} \end{pmatrix} \left(- \frac{(k^2 {v_{\rm A}}^2 - \omega^2)\frac{\rho_0}{\rho_1} - \omega^2 \tanh kx_0}{(k^2 {v_{\rm A}}^2 - \omega^2)\frac{\rho_0}{\rho_1} \tanh kx_0 - \omega^2} \right), \tag{3.10}$$

which can be solved for $v_{\rm A}$ to give

$$v_{\rm A}^2 = \frac{\omega^2}{k^2} \left[1 + \frac{\rho_1}{\rho_0} \begin{pmatrix} \tanh \\ \coth \end{pmatrix} (k(x_0 + \Delta_{\min})) \right]. \tag{3.11}$$

3.4. Low-beta approximation

In a low-beta plasma, the minimum perturbation shift for a quasi-sausage mode (top) and quasi-kink (bottom) is given by

$$\Delta_{\min} = \frac{1}{k} \begin{pmatrix} \tanh^{-1} \\ \coth^{-1} \end{pmatrix} \left(- \frac{(k^2 {v_{\rm A}}^2 - \omega^2) m_1 \frac{\rho_0}{\rho_1} - \omega^2 k \tanh kx_0}{(k^2 {v_{\rm A}}^2 - \omega^2) m_1 \frac{\rho_0}{\rho_1} \tanh kx_0 - \omega^2 k} \right), \tag{3.12}$$

which can be solved for $v_{\rm A}$ to give

$$v_{\rm A}^2 = \frac{\omega^2}{k^2} \left[1 + \frac{k\rho_1}{m_1 \rho_0} \begin{pmatrix} \tanh \\ \coth \end{pmatrix} (k(x_0 + \Delta_{\min})) \right]. \tag{3.13}$$

Table 1. Magneto-seismological application using the amplitude ratio, $R_{\rm A}$, to approximate the Alfvén speed, $v_{\rm A}$.

Type	Mode	Approximation of $k^2 v_{\rm A}^2/\omega^2$ using amplitude ratio, $R_{\rm A}$		
		Thin slab	Incompressible	Low-beta
Surface	Quasi-sausage	$1+\frac{1}{x_0}\left(\frac{R_{\rm A}\frac{\rho_2}{\rho_0 m_2}+\frac{\rho_1}{\rho_0 m_1}}{R_{\rm A}+1}\right)$	$1+\left(\frac{R_{\rm A}\frac{\rho_2}{\rho_0}+\frac{\rho_1}{\rho_0}}{R_{\rm A}+1}\right)\coth kx_0$	$1+k\left(\frac{R_{\rm A}\frac{\rho_2}{\rho_0 m_2}+\frac{\rho_1}{\rho_0 m_1}}{R_{\rm A}+1}\right)\coth kx_0$
	Quasi-kink	$1+k^2x_0\left(\frac{R_{\rm A}\frac{\rho_2}{\rho_0 m_2}-\frac{\rho_1}{\rho_0 m_1}}{R_{\rm A}-1}\right)$	$1+\left(\frac{R_{\rm A}\frac{\rho_2}{\rho_0}-\frac{\rho_1}{\rho_0}}{R_{\rm A}-1}\right)\tanh kx_0$	$1+k\left(\frac{R_{\rm A}\frac{\rho_2}{\rho_0 m_2}-\frac{\rho_1}{\rho_0 m_1}}{R_{\rm A}-1}\right)\tanh kx_0$

Table 2. Magneto-seismological application using the minimum perturbation shift, $\Delta_{\rm min}$, to approximate the Alfvén speed, $v_{\rm A}$.

Type	Mode	Approximation of $k^2 v_{\rm A}^2/\omega^2$ using minimum perturbation shift, $\Delta_{\rm min}$		
		Thin slab	Incompressible	Low-beta
Surface	Quasi-sausage	$\frac{\rho_1}{\rho_0 m_1}(x_0+\Delta_{\rm min})+\frac{1}{1+(\omega/kc_0)^2}+k^2x_0\Delta_{\rm min}$	$1+\frac{\rho_1}{\rho_0}\tanh k(x_0+\Delta_{\rm min})$	$1+\frac{k\rho_1}{m_1\rho_0}\tanh k(x_0+\Delta_{\rm min})$
	Quasi-kink	$\frac{-b\pm\sqrt{b^2-4ac}}{2a}$, defined in text	$1+\frac{\rho_1}{\rho_0}\coth k(x_0+\Delta_{\rm min})$	$1+\frac{k\rho_1}{m_1\rho_0}\coth k(x_0+\Delta_{\rm min})$

4. Discussion

We have introduced the amplitude ratio method and the minimum perturbation shift which quantify the spatial asymmetry in magnetic slab eigenmodes. These expressions can be solved for the Alfvén speed, for a given set of observed parameters, giving us a novel method diagnosing information about the background plasma, thus advancing the field of spatial magneto-seismology.

A summary of the analytical expressions for estimating the Alfvén speed, v_{A}, within a magnetic slab is given in Tables 1 and 2, utilising the amplitude method and the minimum perturbation shift methods, respectively. In practice, a numerical procedure could be made relatively simple and computationally inexpensive by making use of a standard root finding method once the observed parameters have been prescribed but in some cases it might be valid to use an analytical solution from Tables 1 and 2 under the necessary approximation.

Figure 4 illustrates the dependency of the amplitude ratio and minimum perturbation shift on the (non-dimensionalised) slab width, kx_0, and the density ratio, ρ_1/ρ_0, of one external plasma density to the slab density, holding the other external density fixed. varying one density ratio in this way is equivalent to changing the asymmetry of the system. The amplitude ratio is positive (negative) for quasi-kink (quasi-sausage) modes, because the oscillations on each boundary are in phase (anti-phase). Figures 4a and 4b further show that, for a given background parameter regime, the boundary with the highest amplitude is different for quasi-kink and quasi-sausage modes. This is demonstrated by the value of the absolute value of the amplitude ratio being greater than 1 for quasi-sausage modes when it is less than 1 for quasi-kink modes, and *vice versa*. This is in agreement with the properties of the eigenmodes of the analogous spring-mass system introduced by Allcock and Erdélyi (2017). Figures 4c and 4d demonstrate that the position of minimum perturbation for quasi-kink modes is shifted in the opposite direction to that of quasi-sausage modes.

There are a number of ways that the amplitude ratio or minimum perturbation shift can be used for spatial seismology. Firstly, and most simply, given observed values for the wave frequency parameters (frequency or period and wavenumber or wavelength), the background parameters (plasma density inside and in each external side of the slab, which can then be used to determine the sound speeds by assuming equilibrium pressure balance across the slab boundaries), the spatial structure parameters (slab width), and a spatial diagnostic parameter (amplitude ratio or minimum perturbation shift), we can invert the corresponding expression for the spatial wave distribution parameter, Equation (2.21), (2.22), (3.3), or (3.4), to estimate the Alfvén speed. Note that the particular wave mode observed must be known or decomposed from the superposition of modes that are observed.

It is often the case than not all the non-magnetic parameters are well-observable. In this case, the dispersion relation can be solved simultaneously with the equation for the amplitude ratio or the minimum perturbation shift to approximate the Alfvén speed and another unknown parameter. For example, Figure 5 shows the inversion curves for a particular parameter regime typical of a slow surface mode, plotted by prescribing (as if they were observed quantities) all parameters apart from the Alfvén speed, v_{A}, and one of the density ratios, ρ_1/ρ_0, then numerically solving the dispersion relation, Equation (2.6), and expressions for

The amplitude ratio has a strong sensitivity to the changes in the external densities, and therefore the external asymmetry, whereas the minimum perturbation shift has a weaker dependency. This means that the amplitude ratio is likely to be a more effective parameter for diagnosing background parameters. Furthermore, observations of the location of the minimum wave power within a solar magnetic slab will be fraught with noise potentially causing the detection of a false minimum. Noise in amplitude ratio measurements is less likely to introduce large errors because the location of the slab boundaries is a more obvious feature and can be identified by the steep gradients in the wavelength of observed light, for example, and is stable to large noise signals.

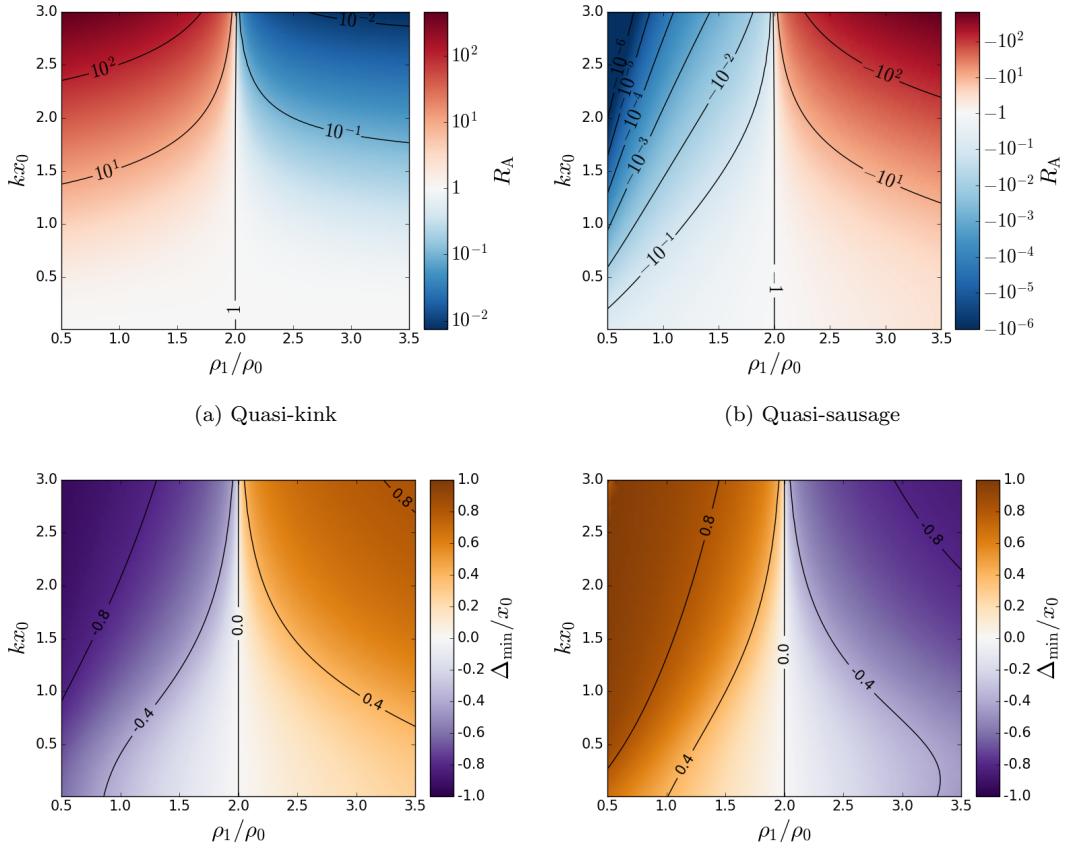

(a) Quasi-kink

(b) Quasi-sausage

(c) Quasi-kink

(d) Quasi-sausage

Figure 4. The amplitude ratio (a, b) and minimum perturbation shift (c, d) as a function of the slab width, non-dimensionalised as kx_0, and the density ratio, ρ_1/ρ_0, for slow quasi-kink (a, c) and quasi-sausage (b, d) surface modes. The other density ratio is set to $\rho_2/\rho_0 = 2$, the characteristic speed ordering inside the slab is $v_A = 1.3c_0$, and the sound speed outside the slab is determined to ensure equilibrium pressure balance.

On a theoretical level, the eigenfunctions of a given system are more sensitive to small changes in the equilibrium parameters than the corresponding eigenfrequencies (Rayleigh-Ritz theorem - references needed, but I cannot find any). This means that spatial seismology techniques are likely to be more effective than temporal techniques.

In future work we would like to determine whether magneto-acoustic waves can be set up in an asymmetric waveguide within the characteristic lifetime of such a structure in the solar atmosphere. This can be established analytically (for linear waves with simple initial conditions) and numerically (for nonlinear waves with more sophisticated initial conditions). Further, a more realistic system, including asymmetric magnetic fields in the external plasmas, or an equilibrium shear flow, would allow for better application to solar waveguides.

Acknowledgments M. Allcock would like to thank the University Prize Scholarship. R. Erdélyi acknowledges the support from the UK Science and Technology Facilities Council (STFC), the Royal Society, and is also grateful to the Chinese Academy of Sciences Presidents International Fellowship Initiative, Grant No. 2016VMA045 for support received.

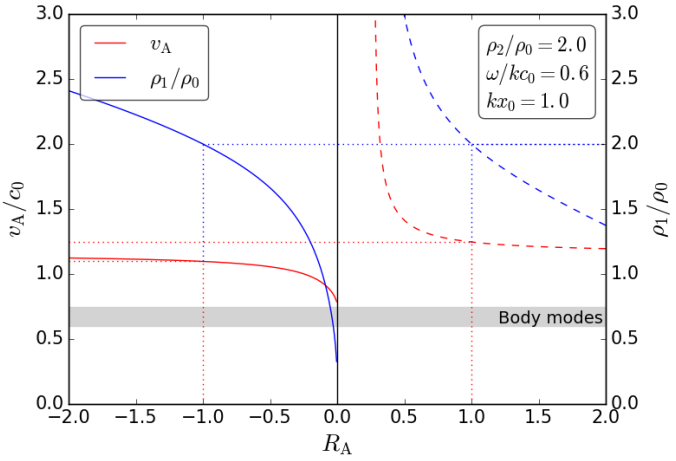

(a) Amplitude ratio inversion.

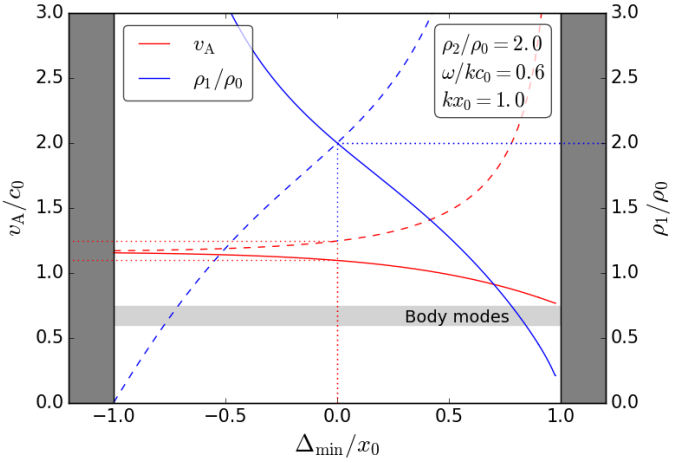

(b) Minimum perturbation shift inversion.

Figure 5. Using prescribed values for the amplitude ratio, R_A, (a) or minimum perturbation shift, Δ_{min}, (b), we can use a numerical inversion to approximate background parameters, in this case the Alfvén speed, v_A, and one of the density ratios, ρ_1/ρ_0. Dashed (solid) lines correspond to the inversion curves for slow quasi-kink (quasi-sausage) surface modes. The dotted lines indicate the inversion for a symmetric slab. The light shaded area indicates the values of the Alfvén speed which correspond to body modes, rather than surface modes, so are not important for SMS. The dark shaded region in Figure (b) illustrates that the minimum perturbation shift must be within the slab, that is $|\Delta_{min}/x_0| < 1$.

Declaration of Potential Conflicts of Interest The authors declare that they have no conflicts of interest.

References

Allcock, M., Erdélyi, R.: 2017, Magnetohydrodynamic Waves in an Asymmetric Magnetic Slab. *Solar Phys.* **292**, 35. DOI. ADS.

Arregui, I.: 2012, Inversion of Physical Parameters in Solar Atmospheric Seismology. *Astrophysics and Space Science Proceedings* **33**, 159. DOI. ADS.

Arregui, I., Oliver, R., Ballester, J.L.: 2012, Prominence Oscillations. *Living Rev. Solar Phys.* **9**, 2. DOI. ADS.

Banerjee, D., Erdélyi, R., Oliver, R., O'Shea, E.: 2007, Present and Future Observing Trends in Atmospheric Magnetoseismology. *Solar Phys.* **246**, 3. DOI. ADS.

De Moortel, I., Nakariakov, V.M.: 2012, Magnetohydrodynamic waves and coronal seismology: an overview of recent results. *Philosophical Transactions of the Royal Society of London Series A* **370**, 3193. DOI. ADS.

Erdélyi, R., Taroyan, Y.: 2008, Hinode EUV spectroscopic observations of coronal oscillations. *Astron. Astrophys.* **489**, L49. DOI. ADS.

Erdélyi, R., Hague, A., Nelson, C.J.: 2014, Effects of Stratification and Flows on P $_1$/ P $_2$ Ratios and Anti-node Shifts Within Closed Loop Structures. *Solar Phys.* **289**, 167. DOI. ADS.

Nakariakov, V.M., Ofman, L.: 2001, Determination of the coronal magnetic field by coronal loop oscillations. *Astron. Astrophys.* **372**, L53. DOI. ADS.

Nakariakov, V.M., Verwichte, E.: 2005, Coronal Waves and Oscillations. *Living Rev. Solar Phys.* **2**, 3. DOI. ADS.

Roberts, B.: 1981a, Wave propagation in a magnetically structured atmosphere. I - Surface waves at a magnetic interface. *Solar Phys.* **69**, 27. DOI. ADS.

Roberts, B.: 1981b, Wave Propagation in a Magnetically Structured Atmosphere. II - Waves in a Magnetic Slab. *Solar Phys.* **69**, 39. DOI. ADS.

Rosenberg, H.: 1970, Evidence for MHD Pulsations in the Solar Corona. *Astron. Astrophys.* **9**, 159. ADS.

Uchida, Y.: 1970, Diagnosis of Coronal Magnetic Structure by Flare-Associated Hydromagnetic Disturbances. *Pub. Astron. Soc. Japan* **22**, 341. ADS.

Verth, G., Van Doorsselaere, T., Erdélyi, R., Goossens, M.: 2007, Spatial magneto-seismology: effect of density stratification on the first harmonic amplitude profile of transversal coronal loop oscillations. *Astron. Astrophys.* **475**, 341. DOI. ADS.

Yang, S., Zhang, J., Erdélyi, R., Hou, Y., Li, X., Yan, L.: 2017, Sunspot Light Walls Suppressed by Nearby Brightenings. *Astrophys. J. Lett.* **843**, L15. DOI. ADS.

Zhang, J., Tian, H., He, J., Wang, L.: 2017, Surge-like Oscillations above Sunspot Light Bridges Driven by Magnetoacoustic Shocks. *Astrophys. J.* **838**, 2. DOI. ADS.